Lead-free acoustic emission sensors

K. H. Lam,[a] D. M. Lin, and H. L. W. Chan
Department of Applied Physics, The Hong Kong Polytechnic University, Hunghom, Hong Kong, China
and Materials Research Centre, The Hong Kong Polytechnic University, Hunghom, Hong Kong, China

(Received 2 September 2007; accepted 28 October 2007; published online 28 November 2007)

Acoustic emission (AE) sensors have been fabricated using both soft- and hard-type lead-free $(Na_{0.5}K_{0.5})NbO_3$-based ceramics. The acoustic and electromechanical properties of the ceramics have been determined using the resonance technique. The lead-free AE sensors were calibrated using a laser source and compared to a commercial sensor. A lead zirconate titanate (PZT) 5*H* ceramics AE sensor has also been fabricated and calibrated for comparison. It was found that the sensitivity of lead-free AE sensors is comparable to that of the lead-based PZT sensor. To evaluate the sensors for potential application, they have been used in the detection of AE in an impact test. The lead-free sensors can reproduce AE signals accurately without giving artifacts and have potential use in commercial AE systems. © *2007 American Institute of Physics.*
[DOI: 10.1063/1.2814024]

I. INTRODUCTION

Acoustic emission (AE) is a transient elastic wave generated by sudden deformation taking place in materials and structures under stress. It is a powerful technology that can be deployed within a wide range of usable applications of nondestructive testing: e.g., for piping systems, reactors, civil structures, etc.[1–3]

In general, AE sensors are used to detect the dynamic motion of waves resulting from acoustic emission and then convert the detected motion into an electrical signal. Previously, copolymers, shape memory alloys, and ceramic/polymer composites have been proposed as the sensing elements of AE sensors.[4–6] Nevertheless, most AE measurements were studied with piezoelectric ceramic sensors. It was proven that the piezoelectric ceramics are appropriate materials for AE testing because of their relatively low cost and high sensitivity.

The most widely used piezoelectric ceramics are lead-based ceramics, especially $Pb(Zr,Ti)O_3$ (PZT), because of their superior piezoelectric properties. Recently, with concern in the environmental pollution of PbO evaporation, it is desirable to use lead-free materials for environmental protection. Lead-free piezoelectric ceramics have attracted considerable interest to replace the lead-based material systems.[7–9] $Bi_{0.5}Na_{0.5}TiO_3$ (BNT) is considered to be one of the good candidates of lead-free piezoelectric ceramics because of its large remnant polarization.[10] However, due to their high coercive field, pure BNT ceramics are difficult to pole and possess lower piezoelectric properties compared with PZT ceramics. In order to improve the properties of BNT ceramics, new $[Bi_{0.5}(Na_{1-x-y}K_xLi_y)_{0.5}]TiO_3$ lead-free piezoelectric ceramics were proposed.[11,12] The partial substitution of Na^+ by K^+ and Li^+ effectively decreases the coercive field of the ceramics, while the strong ferroelectricity is still maintained with good piezoelectric properties. With different dopants, $(K,Na)NbO_3$ (KNN)-based ceramics can be modified to form soft- and hard-type ceramics with reasonably good performance.[12,13] Since the KNN-based ceramics have no low depolarization temperature but only the high Curie temperature, it would be useful for stable performance in applications. In this study, both soft-type and hard-type $(K,Na)NbO_3$-based ceramics were fabricated and used as sensing elements of the AE sensors.

II. MATERIALS

There are two types of KNN-based ceramics used as the sensing elements of the AE sensors: $(Na_{0.5}K_{0.5})NbO_3-0.06Ba(Ti_{0.95}Zr_{0.05})O_3+1$ mol % MnO_2 (KNN-BZT) and $(Na_{0.5}K_{0.5})NbO_3+1$ mol % CuO (KNN-Cu).[14] Both ceramics were prepared by the conventional mixed oxide technique using analytical-grade metal oxides or carbonate powders as raw materials. The powders in the stoichiometric ratio of $K_{0.5}Na_{0.5}NbO_3$ were first mixed and calcined at 880 °C for 6 h by solid-state reaction. Then, the dopants were weighed according to the molar ratios in the above formula and then ball milled for 8 h. The resulting powders were mixed thoroughly with a polyvinyl acetate binder solution and then pressed into disks of 13 mm diameter and 1.3 mm thickness. After removal of the binder, the KNN-BZT and KNN-Cu samples were sintered at 1140–1160 and 1100–1120 °C for 4 h in air, respectively. Fired-on silver slurry was used as electrodes. The sample was poled across the thickness under a dc electric field of 6 kV/mm for 30 min in silicone oil at 200 °C. After poling, the samples were short-circuit annealed at room temperature for 8 h to remove the injected charges. For comparison, PZT 5*H* ceramic disks with similar dimensions have also been fabricated.

The density ρ of the samples was measured using a method based on the Archimedes principle. The piezoelectric coefficient d_{33} of the ceramic disk was measured by a d_{33}

[a]FAX: +852-2333-7629. Electronic mail: kokokh.lam@polyu.edu.hk.

TABLE I. Properties of various sensing elements of the AE sensor.

	PZT 5H	KNN-BZT	KNN-Cu
Density (kg/m^3)	7600	4400	4500
Poling field (kV/mm)	3	6	6
Poling temperature (°C)	120	200	200
Poling time (min)	30	30	30
d_{33} ($\times 10^{-12}$ C/N)	550	200	75
$\varepsilon^T{}_{33}$ at 1 kHz	3400	1100	250
k_t	0.50	0.47	0.46
k_p	0.62	0.48	0.42
g_{33} ($\times 10^{-3}$ V m/N)	18.3	20.5	33.9
Q_M	70	50	800
N_p (Hz m)	1980	3085	3718
N_t (Hz m)	2200	2750	3400
Z_a (MRayl)	35.1	34.2	33.8

meter (ZJ-3B) supplied by the Beijing Institute of Acoustics, Academia Sinica. The electromechanical coupling coefficients (k_t and k_p), mechanical quality factor Q_M, frequency constants (N_p and N_t), and acoustic impedance Z_a of the samples were determined at room temperature following the IEEE standard on piezoelectricity.[15] The dielectric properties of the ceramics were measured using an impedance/gain phase analyzer (Agilent 4294A). The properties of the ceramics are shown in Table I.

As expected, the piezoelectric d coefficient of the PZT sample is higher than that of the lead-free ceramics. Nevertheless, the density and relative permittivity of the lead-free ceramics are much lower than those of PZT ceramics and they have reasonably good electromechanical coupling coefficients. With low relative permittivity, the lead-free samples have relatively high piezoelectric voltage coefficient g_{33} which is a key parameter for being an appropriate sensing material. Among the lead-free ceramics, the KNN-BZT ceramics is the soft type, which has relative high d_{33} and $\varepsilon^T{}_{33}$ with low Q_M. On the other hand, the KNN-Cu sample shows a relatively high Q_M with low d_{33} and $\varepsilon^T{}_{33}$ which is a hard-type ceramics.

III. AE SENSORS

A schematic diagram of the AE sensor is shown in Fig. 1. The ceramic disk was attached inside the aluminum housing (a diameter of 16 mm and a thickness of 6 mm) using a silver epoxy. A coaxial cable was used as an electrical connection to bring the signal out. Figure 2 shows a photograph of the AE sensor.

A commercial broadband AE sensor supplied by Physical Acoustics (model no. S9220) was used to calibrate the

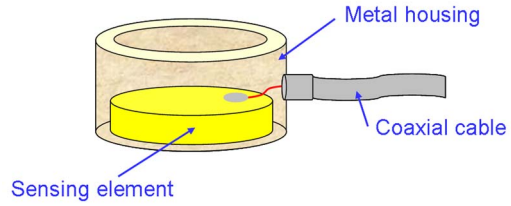

FIG. 1. (Color online) Schematic diagram of the AE sensor.

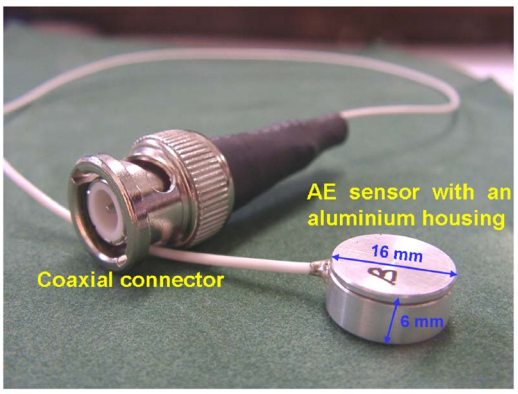

FIG. 2. (Color online) Photograph of the AE sensor in aluminum housing.

homemade sensors. The calibration yields the frequency response of a sensor to waves generated by a laser impact on a metal surface. The voltage response of the sensor is determined at discrete frequency intervals of approximately up to 1.25 MHz by comparing the signal with that received by a commercial sensor with known sensitivity given by the company.

Figure 3 shows the experimental setup of the calibration of the AE sensors with a laser source (neodymium doped yttrium aluminum garnet laser, Spectra-Physics GCR 16). The lens in front of the metal block is used to focus the laser on the metal block surface. During the calibration, the AE sensor was placed 5 cm from the laser impact point on the metal block. To ensure a good acoustic coupling, a thin layer of wax was applied between the sensor and the metal block. Once the laser impinges on the metal block, the wave form $D(t)$ generated from the sensor was amplified using a low-noise preamplifier (Stanford Research Systems, SR560) and then captured using a digital storage oscilloscope (HP Infinium), as shown in Fig. 4. A preamplifier gain of 20 was used throughout the experiments. For calibration, similar experiments have been done with the commercial and homemade AE sensors. The wave forms were then fast Fourier transformed to determine the frequency spectra $D(f)$. The response of the homemade sensors, $M_u(f)$, with respect to that of the standard (commercial) sensor $M_s(f)$, is as follows:

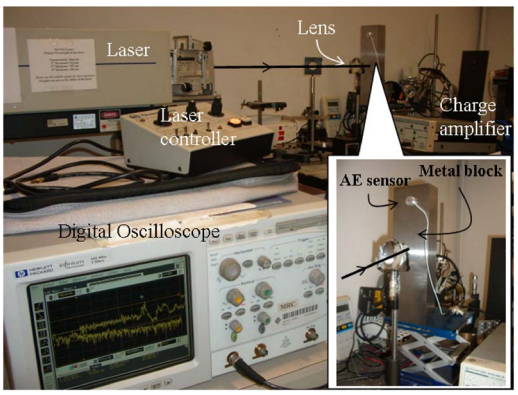

FIG. 3. (Color online) Experimental setup of the calibration of the AE sensor.

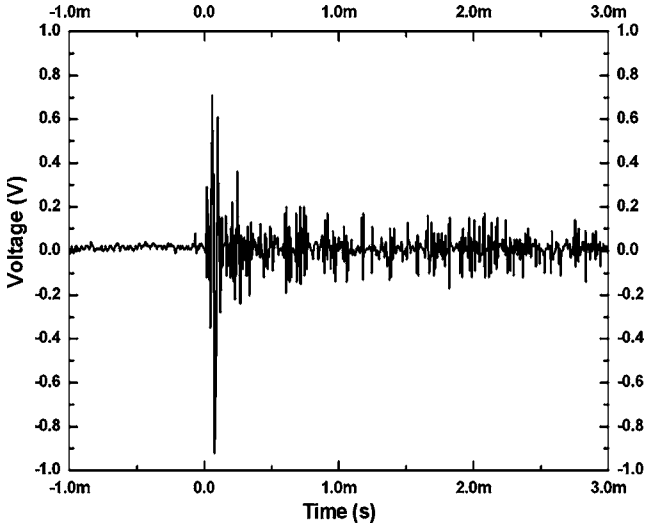

FIG. 4. Voltage vs time wave form of the commercial S9220 AE sensor.

$$M_u(f) = \frac{D_u(f)}{D_s(f)} \times M_s(f), \quad (1)$$

where the subscripts u and s stand for the unknown and standard sensors, respectively. Figure 5 shows the sensitivities of the AE sensors fabricated using KNN-BZT, KNN-Cu, and PZT. It can be seen that the lead-free sensors have the sensitivity comparable to the PZT sensor. This may be due to a high voltage coefficient g of the lead-free ceramics. In the frequency range of 150–400 kHz where most of the AE events are likely to occur, the sensitivity of the sensors approaches 55, even the sensing element consists of lead-free ceramics.

IV. EVALUATION OF AE SENSORS

Besides calibrated using the laser source, the AE sensors were also evaluated for potential application in the detection of impact signals produced by a hammer test. During the measurements, the AE sensor under test was mounted at a designated position on the steel block. The experimental setup is similar to that shown in Fig. 3, and the only difference is the source of impact which was produced by a hammer, as shown in Fig. 6. Since the hammer test was a low-frequency measurement, a low-frequency commercial sensor (model: PICO) was chosen for comparison. Figure 7 compares the detected signals in time domain from KNN-BZT and the PICO sensors (inset). It is shown that the peak amplitude of the lead-free sensor is much higher than that of the commercial sensor with similar signal pattern. It may be due to the relative large area and low electrical impedance of the homemade sensing elements. The low-frequency response of the KNN-BZT, KNN-Cu, and PZT AE sensors is compared in Fig. 8. The lead-free sensors still have sensitivity comparable to that of PZT sensor.

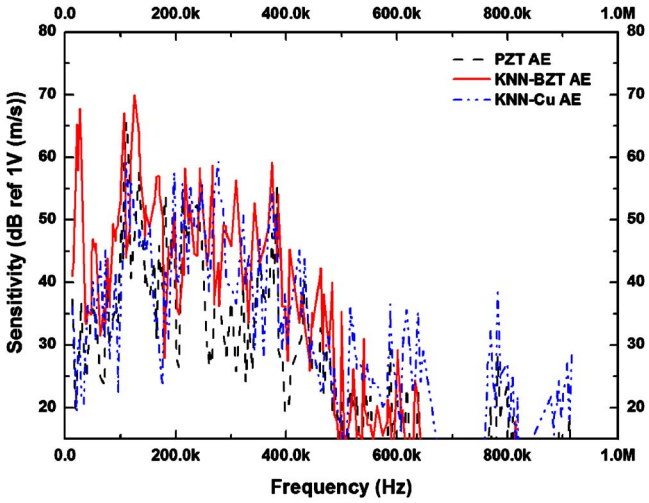

FIG. 5. (Color online) The sensitivity curves of the KNN-BZT, KNN-Cu, and PZT AE sensors as a function of frequency.

FIG. 6. (Color online) Experimental setup of the evaluation of the AE sensor.

V. CONCLUSIONS

Acoustic emission sensors fabricated using lead-free ceramics have been fabricated and characterized. They show comparable sensitivity with the lead-based sensor in both the broadband laser calibration and low-frequency impact test.

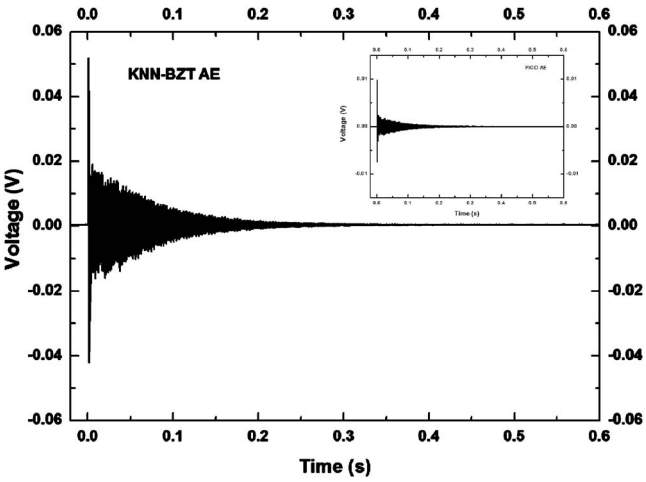

FIG. 7. Voltage vs time wave form of the KNN-BZT AE sensor (inset: a wave form of the commercial PICO AE sensor).

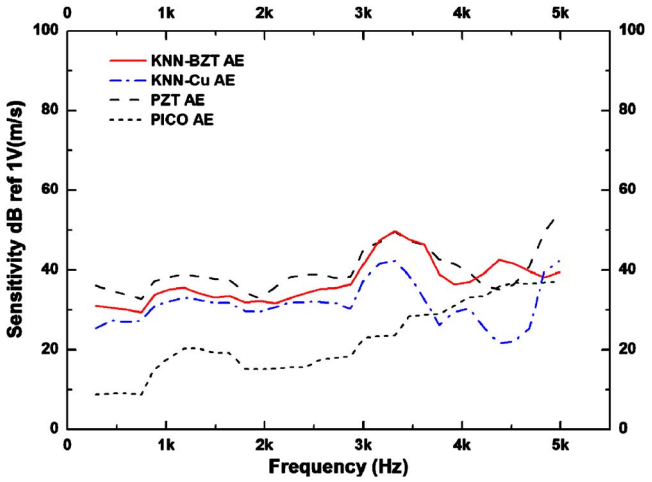

FIG. 8. (Color online) The sensitivity curves of the KNN-BZT, KNN-Cu, PZT AE, and the commercial PICO sensors as a function of frequency.

Both the soft- and hard-type KNN-based lead-free ceramics with high g coefficients have the potential to be used in commercial AE systems.

ACKNOWLEDGMENTS

This work was supported by a grant from the Research Grants Council of the Hong Kong Special Administrative Region (Project No. PolyU 5317/04E) and the Centre for Smart Materials of the Hong Kong Polytechnic University. Supports from the PolyU internal grants (1-BBZ3 and 1-BB95) are also acknowledged.

[1] E. Haque, A. B. Darus, M. M. Yaacob, and F. Ahmed, Proceedings of the 1997 International Conference on Information, Communications and Signal Processing, 1997 (unpublished), Vol. 2, p. 745.
[2] C. U. Grosse, H. W. Reinhardt, and F. Finck, Coll. Math. J. **15**, 274 (2003).
[3] H. Chan, E. Han, J. Q. Wang, and W. Ke, J. Mater. Sci. **40**, 5669 (2005).
[4] R. Stiffler and E. G. Henneke, Mater. Eval. **41**, 956 (1983).
[5] R. Oishi, and H. Nagai, Sens. Actuators, A **22**, 39 (2005).
[6] W. K. Sakamoto, J. A. Malmonge, L. F. Malmonge, and A. F. G. da Silva, IEEE Trans. Dielectr. Electr. Insul. **13**, 1177 (2006).
[7] H. Nagata, M. Yoshida, Y. Makiuchi, and T. Takenaka, Jpn. J. Appl. Phys., Part 1 **42**, 7401 (2003).
[8] Y. Saito, H. Takao, T. Tani, T. Nonoyama, K. Takatori, T. Homma, T. Nagaya, and M. Nakamura, Nature (London) **432**, 84 (2004).
[9] M. D. Maeder, D. Damjanovic, and N. Setter, J. Electroceram. **13**, 385 (2004).
[10] T. Takenaka, K. I. Maruyama, and K. Sakata, Jpn. J. Appl. Phys., Part 1 **30**, 2236 (1991).
[11] C. W. Ahn, H. C. Song, S. Nahm, S. H. Park, K. Uchino, S. Priya, H. G. Lee, and N. K. Kang, Jpn. J. Appl. Phys., Part 1 **44**, L1361 (2005).
[12] S. J. Zhang, R. Xia, T. R. Shrout, G. Z. Zang, and J. F. Wang, J. Appl. Phys. **100**, 104108 (2006).
[13] M. Matsubara, K. Kikuta, and S. Hirano, J. Appl. Phys. **97**, 114105 (2005).
[14] D. M. Lin, K. W. Kwok, and H. L. W. Chan, Appl. Phys. Lett. **90**, 232903 (2007).
[15] IEEE standard on piezoelectricity, ANSI/IEEE Std. 176 (1987).